Neuron, Vol. 27, 45–56, July, 2000, Copyright ©2000 by Cell Press

Timing-Based LTP and LTD at Vertical Inputs to Layer II/III Pyramidal Cells in Rat Barrel Cortex

Daniel E. Feldman*
Neural Development Section
National Institute of Neurological Disorders and Stroke
National Institutes of Health
Bethesda, Maryland 20892

Summary

Experience-dependent plasticity in somatosensory (S1) and visual (V1) cortex involves rapid depression of responses to a deprived sensory input (a closed eye or a trimmed whisker). Such depression occurs first in layer II/III and may reflect plasticity at vertical inputs from layer IV to layer II/III pyramids. Here, I describe a timing-based, associative form of long-term potentiation and depression (LTP/LTD) at this synapse in S1. LTP occurred when excitatory postsynaptic potentials (EPSPs) led single postsynaptic action potentials (APs) within a narrow temporal window, and LTD occurred when APs led EPSPs within a significantly broader window. This long LTD window is unusual among timing-based learning rules and causes EPSPs that are uncorrelated with postsynaptic APs to become depressed. This behavior suggests a simple model for depression of deprived sensory responses in S1 and V1.

Introduction

Experience dramatically changes sensory maps in primary somatosensory (S1) and visual (V1) cortex (Kaas, 1991; Kossut, 1992; Buonomano and Merzenich, 1998). In these areas, partial sensory deprivation causes map plasticity that occurs first in layer II/III, and only later, or not at all, in layer IV, suggesting an initial locus for plasticity at intracortical synapses (Diamond et al., 1993, 1994; Glazewski and Fox, 1996; Trachtenberg et al., 2000). Plasticity is widely hypothesized to be driven by correlations between pre- and postsynaptic activity (Hebb, 1949; Stent, 1973; Armstrong-James et al., 1994; Wang et al., 1994) and to involve long-term potentiation and depression (LTP/LTD) of synaptic efficacy (Bear et al., 1987; Miller et al., 1989; Fregnac et al., 1994; Singer, 1995; Buonomano and Merzenich, 1998). However, exactly how LTP and LTD contribute to map plasticity in vivo is unclear.

A prominent early component of plasticity in both S1 and V1 is a rapid depression of neuronal responses to deprived sensory inputs, which often precedes a subsequent increase in responses to spared inputs (Mioche and Singer, 1989; Glazewski and Fox, 1996). This depression has been well described in S1 of young adult rats in which all but a single whisker is plucked for several days to weeks (univibrissa rearing). In normal rats, virtually all layer IV and layer II/III neurons within a given barrel column in S1 respond most strongly to deflection of a single "principal" whisker corresponding to the position of that column within the cortical whisker map. During univibrissa rearing, layer II/III neurons in deprived barrel columns undergo a rapid depression of responses to their principal (plucked) whisker, while layer IV neurons in the same barrel columns do not (Glazewski and Fox, 1996). This principal whisker response depression has been hypothesized to involve LTD at excitatory vertical (within-column) synapses from layer IV to layer II/III, because these synapses are thought to drive principal whisker responses in the upper layers (Armstrong-James et al., 1992).

What type of LTD might be involved is not known. Principal whisker depression is greatest for layer II/III cells immediately adjacent to a spared whisker column, and weakest away from the spared column or when all whiskers are plucked. This result suggests that depression involves heterosynaptic LTD, in which activity on spared pathways drives depression on nearby deprived pathways, as well as homosynaptic LTD driven by spontaneous activity on the deprived pathways themselves (Glazewski et al., 1998). However, heterosynaptic LTD typically requires intense induction protocols that are unlikely to occur in vivo. One alternative model, proposed to explain similar plasticity in V1, is that depression involves homosynaptic LTD governed by a sliding plasticity threshold that imparts heterosynaptic-like behavior (Bienenstock et al., 1982; Rittenhouse et al., 1999). Another possibility, investigated here, is that depression involves "timing-based" LTP and LTD induced by precise temporal associations between excitatory postsynaptic potentials (EPSPs) and postsynaptic action potentials (APs). Such plasticity has been observed recently at several synapses (Linden, 1999) and has powerful Hebbian-like properties (Sejnowski, 1999), but its role in sensory map plasticity is unknown.

In this paper, I describe timing-based LTP and LTD at vertical synapses onto layer II/III pyramids in S1. The temporal windows for inducing LTP and LTD at these synapses are unusual and confer the property that spontaneous activity, if it is poorly correlated with postsynaptic spiking, will robustly drive depression on this pathway. This learning rule is appropriate to explain both homosynaptic and heterosynaptic aspects of principal whisker depression during univibrissa rearing and can also explain the depression of closed eye responses in layer II/III that occurs during monocular deprivation in V1 (Trachtenberg et al., 2000).

Results

Physiological Properties of Excitatory Vertical Inputs onto Layer II/III Pyramidal Cells

Vertical, within-column inputs to layer II/III pyramidal cells were studied in acute slices of S1 using just-suprathreshold extracellular stimulation in layer IV and whole-cell recording in layer II/III pyramidal cells in the same barrel column (Figure 1A). In voltage-clamp recordings, evoked postsynaptic currents consisted either of a single, short-latency inward current at −70 mV or a short-latency current followed by variable, longer-latency inward currents (Figure $1B_1$). In current clamp, similarly

E-mail: dfeldman@codon.nih.gov.

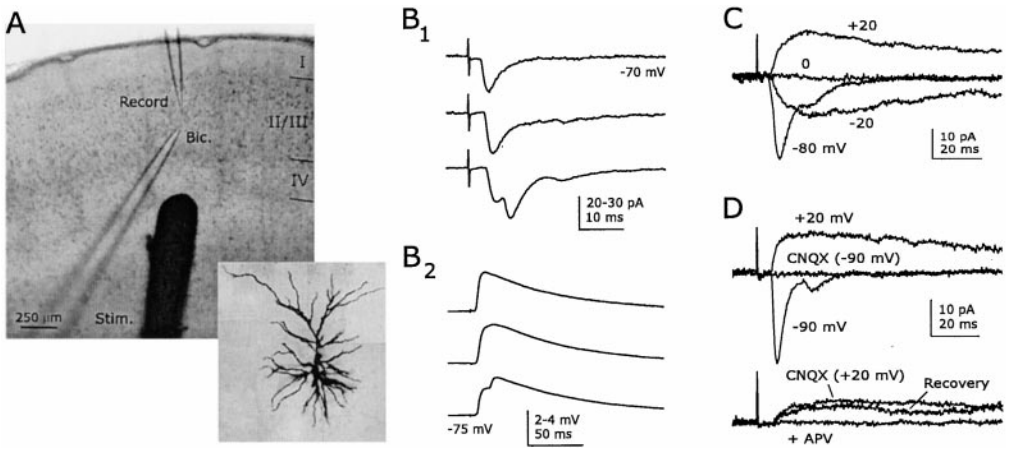

Figure 1. Physiology of Excitatory Vertical Synapses on Layer II/III Pyramidal Cells

(A) Position of stimulation, recording, and bicuculline electrodes relative to barrels in layer IV during an experiment.
(Inset) Biocytin-filled layer II pyramidal cell visualized by avidin-biotin-HRP histochemistry.
(B_1) Representative EPSCs recorded from three pyramidal cells in voltage clamp. $V_{hold} = -70$ mV. Bottom trace shows multicomponent EPSC.
(B_2) Representative EPSPs from three cells in current clamp ($V_{rest} \approx -75$ mV).
(C) Example of EPSC reversal at 0 mV. Holding potential is indicated. A slow NMDA receptor current was prominent at depolarized potentials.
(D) AMPA and NMDA receptor components of the EPSC. A fast AMPA current, prominent at −90 mV, was blocked by 10 μM CNQX. In the same cell, a CNQX-resistant, slower NMDA receptor current was revealed by depolarization to +20 mV and was blocked reversibly by 50 μM D-APV. Traces are means of 20–30 sweeps.

shaped depolarizing PSPs were observed (Figure $1B_2$). The latency of the earliest component was only negligibly affected by increasing stimulation intensity (0.2 ± 0.1 ms, n = 9) or frequency (0.2 ± 0.2 ms, n = 4), suggesting that this component reflects direct monosynaptic input, most likely vertical input from cells in layers IV–VI of the same barrel column (see Experimental Procedures). Only this early component of the response was studied.

Bicuculline methiodide (BMI) was routinely applied focally near the recording site to block γ-aminobutyric acid type A ($GABA_A$) inhibitory postsynaptic currents (IPSCs) without inducing epileptiform activity (Castro-Alamancos et al., 1995). Under these conditions, postsynaptic currents reversed at 0.6 ± 0.9 mV (n = 17), confirming that $GABA_A$ receptors were blocked completely and that currents were EPSCs (Figure 1C). EPSCs had two components with properties characteristic of AMPA and NMDA receptor currents (Hestrin et al., 1990). The AMPA current had rapid kinetics, was prominent at −90 mV, was largely voltage independent, and was completely blocked by 10 μM 6-cyano-7-dinitroquinoxaline-2,3-dione (CNQX; n = 6; Figure 1D). The NMDA current had slower kinetics, was CNQX resistant, was observed only at depolarized potentials, and was reversibly blocked by 50 μM D-APV (n = 8; Figure 1D).

Homosynaptic LTP and LTD Induced by Postsynaptic Depolarization

Homosynaptic LTP and LTD can be induced at vertical inputs to layer II/III pyramids in S1 by high-frequency and low-frequency presynaptic stimulation, respectively (Aroniadou-Anderjaska and Keller, 1995; Castro-Alamancos et al., 1995; Kitagawa et al., 1997). In the hippocampus and V1, these stimulation protocols are thought to induce LTP and LTD by depolarizing the postsynaptic cell to different levels and thereby triggering different postsynaptic Ca^{2+} signals (Lisman, 1989; Artola and Singer, 1993; Malenka and Nicoll, 1993; Cummings et al., 1996). To determine if LTP and LTD could be induced in S1 by pairing release with different levels of postsynaptic depolarization, a standard voltage clamp pairing protocol was applied.

EPSCs were evoked at a constant rate throughout the experiment. After a baseline period in which cells were held at −70 mV, LTP was induced by transiently depolarizing the cell to 0 mV for 50–75 consecutive stimuli without changing the stimulation rate. The cell was then returned to −70 mV, and plasticity was assessed. For the cell in Figure 2A, this protocol increased mean EPSC amplitude from 20.5 pA during the baseline period to 28.1 pA measured 10–15 min after repolarization, an EPSC amplitude ratio of 1.37. Across all cells, the mean EPSC amplitude ratio following LTP was 1.45 ± 0.19 (SEM, n = 8, age: 20–22 d). LTP was stable for the duration of recording (average: 30 min, maximum: 48 min; Figure 2C) and was significant across the cell population ($p < 0.05$, two-tailed, one-sample t test).

To induce LTD, cells were transiently depolarized to −50 mV instead of 0 mV, a procedure that induces LTD at hippocampal and thalamocortical synapses (Feldman et al., 1998; Ngezahayo et al., 2000). In the cell in Figure 2B, the mean EPSC amplitude decreased from 17.1 pA during baseline to 11.2 pA following repolarization, an EPSC amplitude ratio of 0.66. Across all cells, the mean EPSC amplitude ratio after induction of LTD was 0.76 ± 0.06 (n = 11). Like LTP, LTD was stable for the duration of recording (mean: 35 min, maximum: 54 min; Figure 2D) and was significant across the cell population ($p < 0.002$, two-tailed, one-sample t test). There was no correlation between the magnitude of LTD and age (age range: 15–24 d, $r = 0.144$, $p > 0.5$). The average amounts of LTP and LTD were similar to those reported using high- or low-frequency presynaptic stimulation (Lee et al., 1991; Aroniadou-Anderjaska and Keller, 1995; Castro-Alamancos et al., 1995). These results indicate that

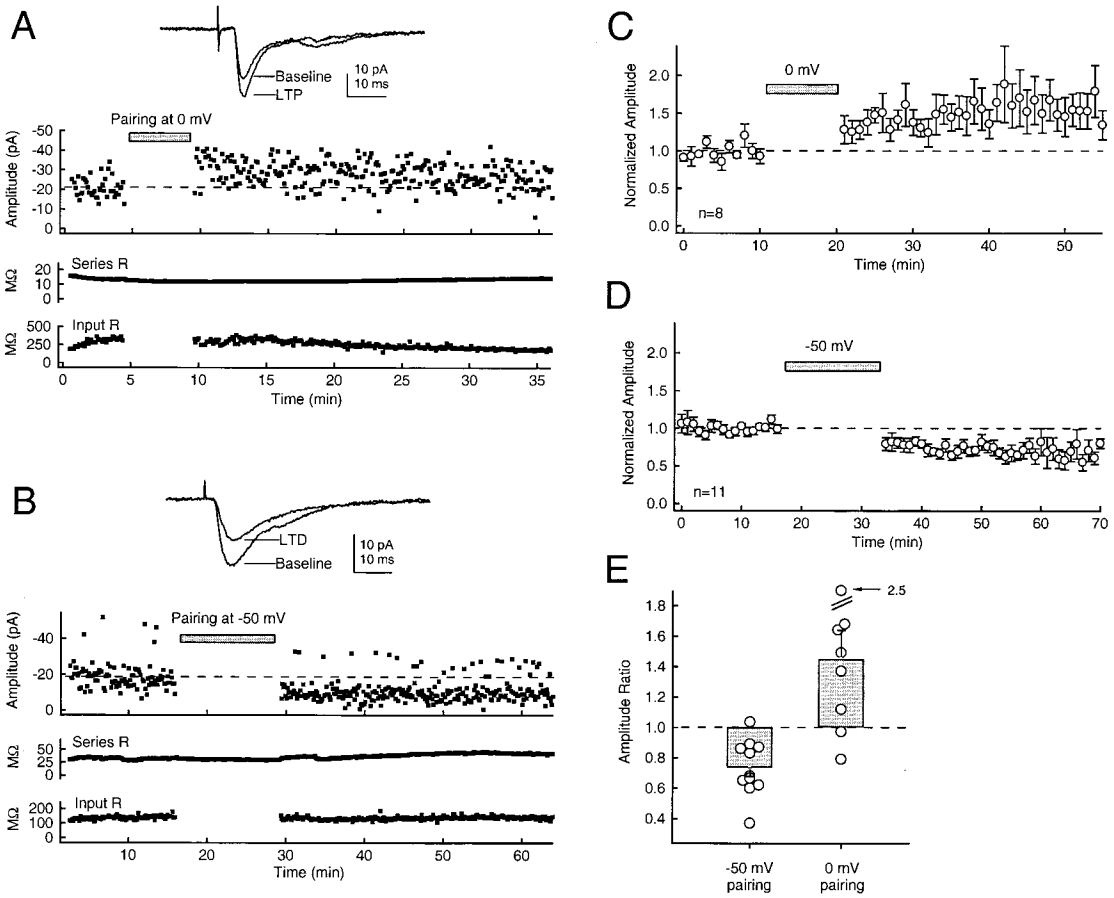

Figure 2. LTP and LTD Induced in Voltage Clamp by Pairing Presynaptic Stimulation with Postsynaptic Depolarization

(A) Experiment showing LTP. After a short baseline period (V_{hold} = −70 mV), the cell was depolarized to 0 mV for 50 stimuli without changing the stimulation rate. Points denote EPSC amplitude for each sweep of the experiment. LTP was apparent upon return to −70 mV as a stable increase in EPSC amplitude without significant changes in R_{input} or R_{series}. Dashed line, mean EPSC amplitude at the end of baseline.

(Inset) Means of 50 EPSCs at the end of the baseline period and beginning 10 min after pairing.

(B) Experiment demonstrating LTD. The protocol was identical to that in (A), except that the cell was depolarized to −50 mV for 100 sweeps to induce LTD.

(C) Mean effect of pairing at 0 mV (eight cells, 50–100 pairing sweeps). Error bars, SEM.

(D) Mean effect of pairing at −50 mV (eleven cells, 100 pairing sweeps).

(E) Amount of LTP or LTD for each cell tested. Bars show mean, and error bars show SEM for each pairing condition.

strong postsynaptic depolarization coincident with presynaptic activity robustly induces LTP at this synapse, while weak postsynaptic depolarization coincident with presynaptic activity induces LTD.

LTP and LTD Induced by AP-EPSP Pairing

Timing-based, associative plasticity was induced in current-clamp experiments by pairing single EPSPs with single postsynaptic APs evoked by current injection through the recording electrode (Figure 3). EPSPs were evoked at a constant rate throughout the experiment. After a stable baseline period, a brief positive current injection (range: 0.5–1.8 nA, mean: 1.4 nA, 5–6 ms duration) was used to evoke a postsynaptic AP at a precise delay preceding or following each EPSP. After 50–100 pairing sweeps, current injection was suspended, and EPSPs were monitored to detect plasticity. Cells were excluded from analysis if the input resistance (mean: 110 MΩ) changed by more than 30% or if the resting membrane potential (mean: −74.6 mV) changed by more than 8 mV; 44 cells met these criteria and were included for analysis.

An example of LTP induced by AP-EPSP pairing is shown in Figure 3A. The average initial slope of the EPSP during the baseline was 0.66 mV/ms. The pairing period consisted of 75 consecutive sweeps in which each EPSP was followed by a postsynaptic AP. The pairing delay was +3 ms (defined as the delay from the onset of the EPSP to the peak of the AP, with positive delays indicating EPSPs leading APs). Pairing caused a stable increase in the initial slope of the EPSP to 0.91 mV/ms, an EPSP slope ratio of 1.38. LTP was not associated with any appreciable changes in input resistance, series resistance, or membrane potential.

LTD was induced when the AP preceded the EPSP during the pairing period (i.e., the pairing delay was negative). In the example in Figure 3B, the pairing delay was −107 ms (AP leading). Pairing caused a stable decrease in the slope of the EPSP from 0.32 mV/ms to 0.25 mV/ms, an EPSP slope ratio of 0.78.

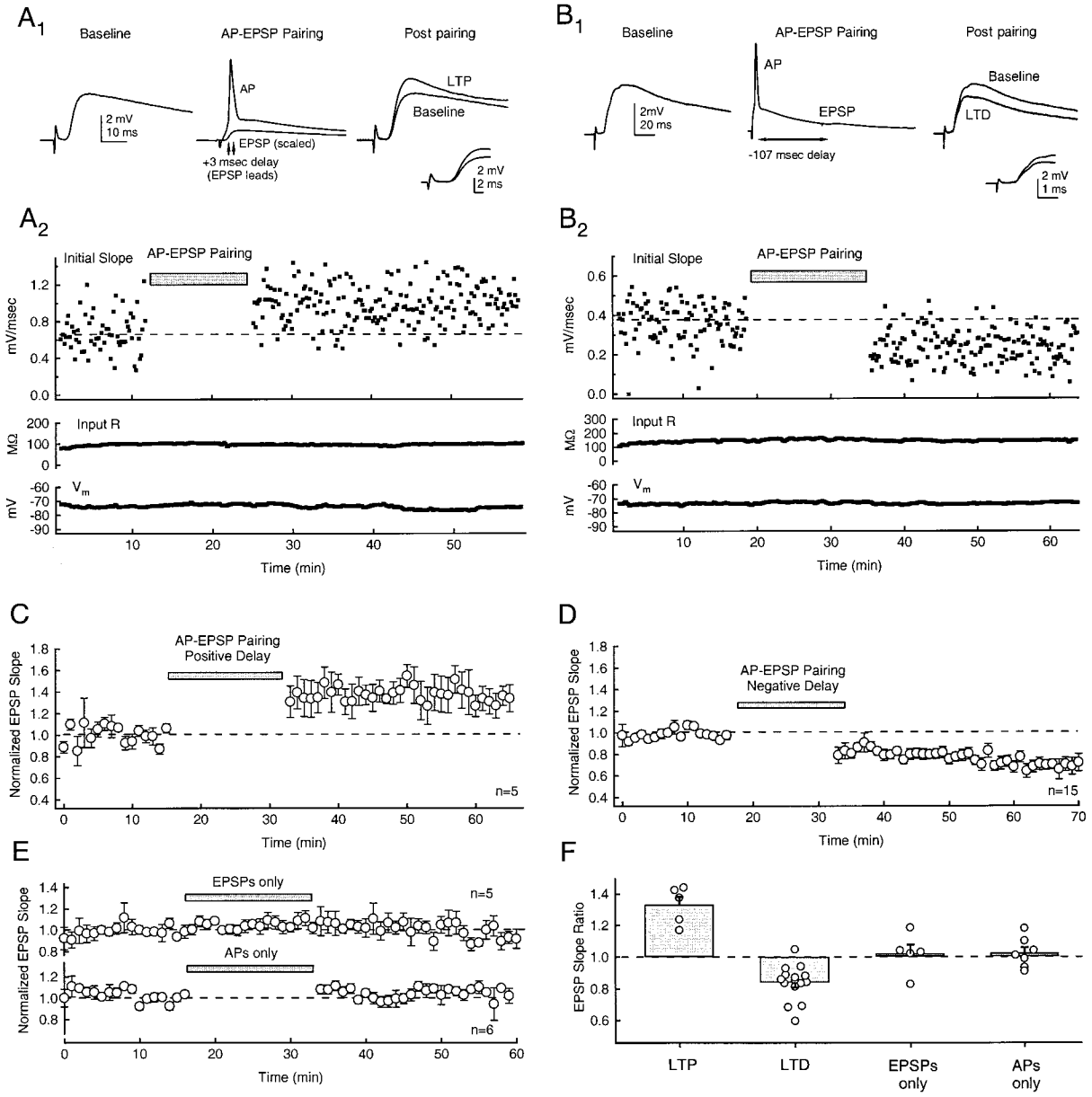

Figure 3. LTP and LTD Induced by AP-EPSP Pairing

(A_1 and A_2) Example of LTP. Points in A_2 denote EPSP initial slope for each sweep (stimulation rate: 0.133 Hz). During pairing, an AP was elicited by somatic current injection (+1.1 nA, 5 ms) after each EPSP. The AP-EPSP delay was +3 ms (EPSP leading). After pairing, LTP was observed without changes in R_{series}, R_{input}, or V_m. Traces in A_1 show average EPSPs for baseline period and a period beginning 10 min after pairing (50 sweeps each). The mean AP during pairing is also shown. Arrowheads indicate EPSP onset and AP peak.

(Inset traces) Change in initial slope with LTP.

(B_1 and B_2) Experiment demonstrating LTD. The protocol was identical to that in (A), except that the AP-EPSP delay during pairing was −107 ms (AP leading).

(C–F) Mean effects of AP-EPSP pairing.

(C) Pairing delays of +3 to +15 ms (EPSP leading, 75–100 pairing sweeps, n = 5 cells). Points show means for 1 min epochs. Error bars, SEM.

(D) Pairing delays of −8 to −50 ms (AP leading, 100 pairing sweeps, n = 15 cells).

(E) Control experiments in which only EPSPs (top, n = 5 cells) or only APs (bottom, n = 6 cells) were evoked during the "pairing" period.

(F) Change in EPSP slope for all cells. Bars show mean ± SEM. Dashed line, no plasticity.

Across cells, LTP was observed consistently with pairing delays of +3 to +15 ms (EPSP leading). The mean EPSP slope ratio after LTP induction was 1.33 ± 0.05 (SEM, n = 5; Figure 3C). LTD was observed most consistently with pairing delays of 0 to −50 ms (AP leading). Occasionally, longer pairing delays (up to −107 ms; Figure 3B) also produced LTD. For all cells tested with pairing delays of −8 to −50 ms, the mean slope ratio was 0.79 ± 0.05 (SEM, n = 15; Figure 3D). Plasticity was not observed when only EPSPs (mean slope ratio

1.02 ± 0.06, n = 5) or only APs (1.01 ± 0.03, n = 6) were elicited during the pairing period (Figure 3E). These results demonstrate that close temporal associations between EPSPs and postsynaptic APs are capable of inducing long-term plasticity at this synapse.

Plasticity Induced by Brief Changes in AP-EPSP Timing

To confirm that brief changes in AP-EPSP timing were sufficient to induce long-term plasticity, 37 neurons were subjected to a "delay change" protocol in which both EPSPs and APs were elicited at a constant rate throughout the experiment, and plasticity was induced simply by transiently changing the relative timing of EPSPs and APs. Figure 4A shows an example in which LTP was induced. An EPSP and an AP were evoked in every sweep of the experiment (0.133 Hz). During the baseline and test periods, the AP followed the EPSP with a delay of +500 ms. During "pairing," the AP-EPSP delay was changed to +9 ms for 40 consecutive sweeps, after which it was returned to +500 ms. This brief change in the AP-EPSP delay was sufficient to induce robust LTP (EPSP slope ratio: 1.77). Using the same protocol, LTD could be induced when the delay was changed transiently such that the AP led the EPSP (e.g., Figure 4B; −49 ms pairing delay, EPSP slope ratio: 0.81).

Across the cell population, changing the delay to 10 ± 1 ms (EPSP leading) induced LTP (mean slope ratio: 1.33 ± 0.07, n = 6; Figure 4C), whereas changing the delay to −20 ± 1 ms (AP leading) induced LTD (mean slope ratio: 0.80 ± 0.04, n = 7; Figure 4D). In contrast, maintaining the AP-EPSP delay at +500 ms, the same delay used in the baseline and test periods, resulted in no significant plasticity (0.97 ± 0.06, n = 5; Figure 4E). Thus, short periods of altered AP-EPSP timing were sufficient to induce long-lasting changes in synaptic efficacy.

Temporal Windows for Induction of LTP and LTD

The relationship between AP-EPSP pairing delay and resulting LTP or LTD is shown in Figure 5. Each point represents a single cell tested with one pairing delay (Figure 5A). LTP was induced reliably by pairing delays of +3 to +14 ms (EPSP leading), while delays of 15 ms or longer failed to elicit LTP. In contrast, robust LTD was induced by negative pairing delays of up to −50 ms (AP leading), and even at a −100 ms delay, two cells showed significant LTD. A pairing delay of −250 ms consistently failed to induce plasticity. For comparison, the variability observed for 16 cells in three sets of control experiments in which plasticity was not induced (cells in Figures 3E and 4E; mean slope ratio: 1.00 ± 0.03) is shown by the dashed lines.

The statistical significance of plasticity at different pairing delays was assessed by dividing the data set into eight pairing delay ranges plus an additional group representing the 16 control cells (Figure 5B). The delay ranges were +60 to +26 ms, +25 to +15 ms, +14 to 0 ms, 0 to −14 ms, −15 to −25 ms, −26 to −60 ms, −90 to −110 ms, and −240 to −260 ms. There was a significant effect of pairing delay on EPSP slope ratio ($p < 0.001$, ANOVA). The effect of each pairing delay was then assessed relative to the control cells using Dunnet's multiple comparison test. At room temperature, significant LTP was observed only for the 0 to +14 ms delay range (mean slope ratio: 1.33 ± 0.07, n = 10, $p < 0.05$). Significant LTD was observed for delays of 0 to −14 ms (mean slope ratio: 0.82 ± 0.07, n = 7, $p < 0.05$), −15 to −25 ms (0.80 ± 0.04, n = 13, $p < 0.05$), and −26 to −60 ms (0.84 ± 0.04, n = 10, $p < .05$). Similar temporal windows for LTP and LTD were observed in a separate group of 13 cells recorded at more physiological temperatures (31°C–33° C; squares in Figure 5A).

Across all cells, there was no significant correlation between age and the magnitude of plasticity for either LTP (3–12 ms pairing delays, n = 13, r = 0.146, $p > 0.5$), LTD at short pairing delays (−8 to −22 ms delays, n = 27, r = 0.158, $p > 0.2$), or LTD at long pairing delays (−39 to −50 ms delays, n = 10, r = 0.043, $p > 0.5$).

Thus, the temporal window for induction of LTD extended to delays of at least −50 ms, whereas the window for induction of LTP included only delays less than +14 ms. This difference, which was unexpected, corresponds to an LTD window that is at least three and a half times longer than the window for LTP.

Depression of EPSPs Uncorrelated with Postsynaptic Spiking

The learning rule in Figure 5 makes an unusual prediction for plasticity in the case of EPSPs that are temporally uncorrelated with postsynaptic APs and that therefore generate random AP-EPSP delays. Because the integral of the LTD window is greater than that of the LTP window, these uncorrelated EPSPs will tend to elicit, on average, more LTD than LTP. Thus, if LTP and LTD sum linearly, synapses generating uncorrelated EPSPs would be predicted to depress over time. This prediction was tested by pairing EPSPs and APs at delays that varied randomly for each sweep of the pairing period (Figure 6). When AP-EPSP delays were varied randomly between −50 and +50 ms during pairing (a range of delays over which the integral of the LTD window was larger than that of the LTP window), significant LTD resulted, consistent with the net induction of more LTD than LTP. An example is shown in Figure 6A. Across cells, the mean slope ratio following this pairing protocol was 0.71 ± 0.12 (n = 7; closed circles in Figure 6B). In contrast, when pairing delays were varied randomly between −10 ms and +10 ms (a range of delays over which LTP and LTD windows have similar integrals), no significant plasticity was observed (mean slope ratio: 0.97 ± 0.06, n = 5; open circles in Figure 6B). This experiment shows directly that synapses that generate EPSPs uncorrelated with postsynaptic APs become depressed over time as a result of the temporally asymmetric windows for LTP and LTD.

Dependence on NMDA Receptors

Homosynaptic LTP and LTD at vertical inputs to layer II/III in S1 require NMDA receptor activation (Castro-Alamancos et al., 1995). To determine whether timing-based plasticity at this synapse was also NMDA receptor dependent, as reported at other synapses (Magee and Johnston, 1997; Markram et al., 1997; Bi and Poo, 1998; Debanne et al., 1998; Zhang et al., 1998), LTP and LTD were attempted using the delay change protocol in the presence of D-APV (50 μM). APV completely blocked induction of LTD (−20 ms pairing delay; mean EPSP slope ratio: 1.04 ± 0.04, n = 7 cells). APV also blocked LTP (+10 ms pairing delay), revealing instead a significant depression (0.81 ± 0.05, n = 6, $p < 0.02$, one-sample t test versus mean of 1.0). Stable EPSPs

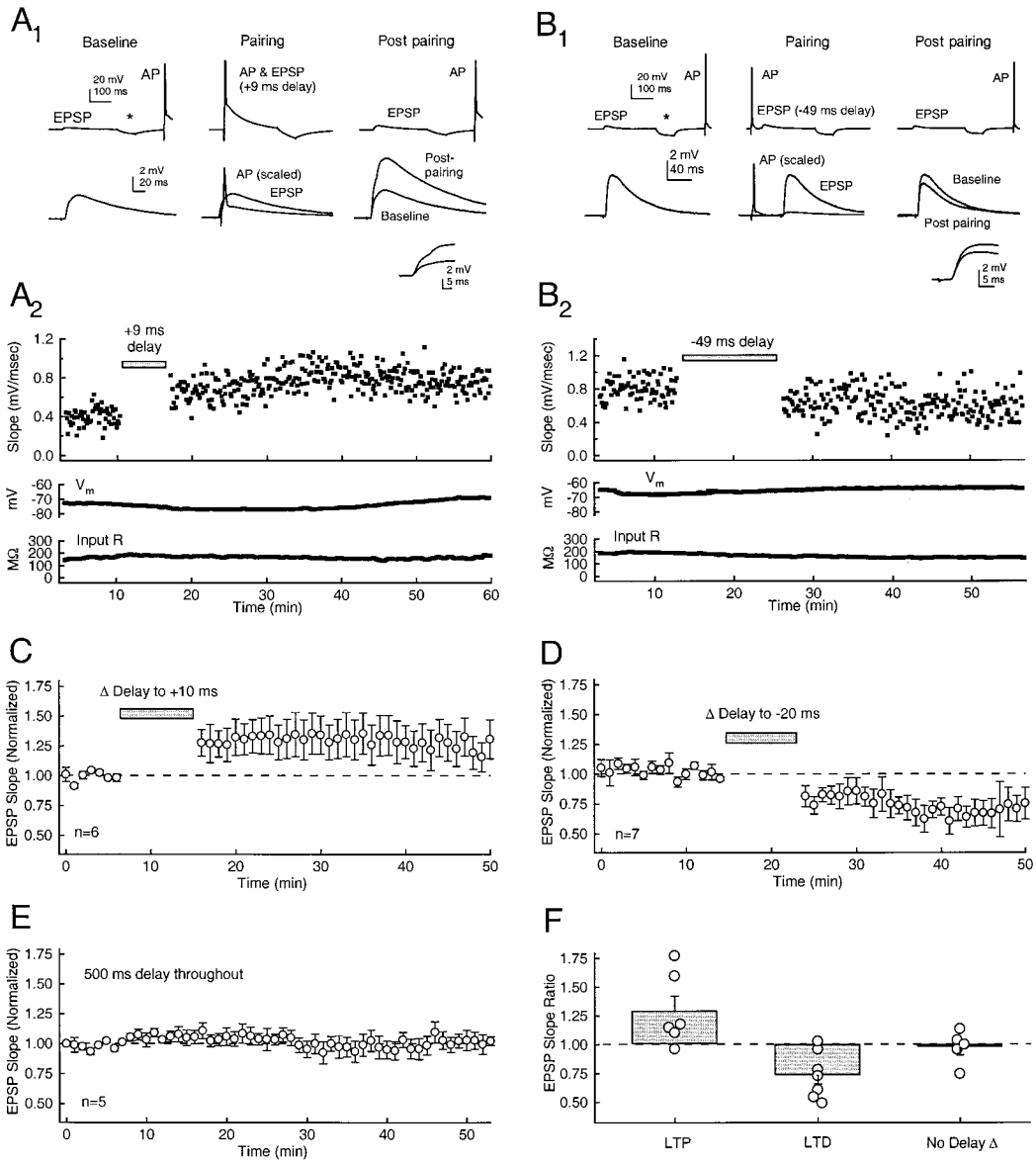

Figure 4. LTP and LTD Induced by Transient Changes in AP-EPSP Timing

(A) Example of LTP.

(A_{1}) Top row, mean traces (50 sweeps each) showing EPSP, AP, and current pulse for measuring R_{input} (asterisk) in different epochs of the experiment. Bottom row, EPSPs enlarged from the upper traces.

(Inset traces) Initial slope of the EPSP before and after pairing, demonstrating LTP.

(A_{2}) EPSP initial slope during baseline and postpairing periods, when the AP-EPSP delay was +500 ms. During pairing, the AP-EPSP delay was shifted to +9 ms for 40 sweeps.

(B) Example of LTD. The same protocol was used as in (A), except that during pairing, the AP-EPSP delay was shifted from +500 ms to −49 ms (AP leading) for 100 sweeps.

(C) Mean effect of changing the AP-EPSP delay to +10 ms (40–100 sweeps, n = 6 cells).

(D) Mean effect of changing the delay to −20 ms (100 sweeps, n = 7 cells).

(E) Control experiments in which a +500 ms delay was maintained throughout the experiment.

(F) Change in EPSP slope for each cell. Bars show mean ± SEM.

were observed in control experiments in which a constant delay of +500 ms was maintained throughout the 50 min experiment in the presence of APV (EPSP slope ratio 1.03 ± 0.09, n = 4). Thus, LTP and LTD induced by AP-EPSP pairing at this synapse required NMDA receptor activation. However, when NMDA receptors were blocked by APV, positive pairing delays produced an additional NMDA receptor–independent form of LTD.

Disinhibition Is Not Required for Plasticity

In the experiments reported above, inhibition was blocked with BMI to allow EPSPs to be studied in isolation. However, disinhibition was not required for induc-

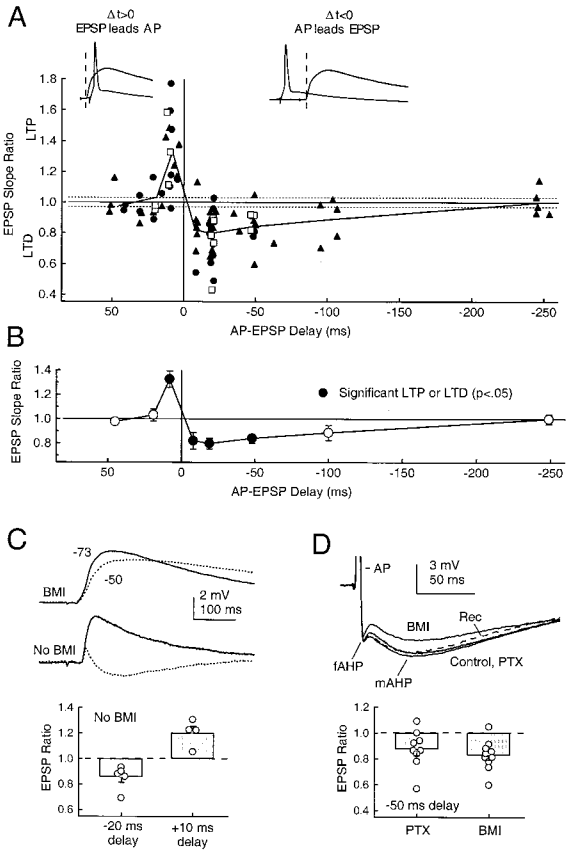

Figure 5. Temporal Windows for Induction of LTP and LTD by AP-EPSP Pairing

(A) EPSP slope ratio for each cell tested, as a function of AP-EPSP delay during pairing. Triangles, standard AP-EPSP pairing protocol at 20°C–23°C. Closed circles, delay change protocol at 20°C–23°C. Squares, delay change protocol at 32° ± 1°C. Lines connect mean slope ratios for different ranges of pairing delays (see text). $\Delta t > 0$ indicates positive delays, and $\Delta t < 0$ indicates negative delays. Dashed lines, ±SEM for cells in control experiments (n = 16).

(B) Mean EPSP slope ratio for the different ranges of pairing delays. Closed points show delays that produced EPSP slope ratios significantly different from those in control experiments.

(C) Plasticity does not require disinhibition. Top, PSPs from representative cells with and without BMI (solid traces, $V_m = -73$ mV; dotted traces, $V_m = -50$ mV). With BMI, depolarization lengthened EPSPs, consistent with NMDA receptor activation, but revealed no IPSPs. Without BMI, depolarization often revealed early EPSPs followed by later, hyperpolarizing IPSPs. Bottom, effect of AP-EPSP pairing for all cells tested without BMI. Bars show mean ± SEM.

(D) The long window for LTD induction is not due to blockade of AHPs by BMI. Top, BMI but not PTX reduces the mAHP in a representative cell. Traces are means of 10–15 sweeps. Bottom, AP-EPSP pairing at −50 ms delays induced significant LTD in the presence of both PTX and BMI. BMI data are from experiments in Figures 3 and 4. Abbreviations: fAHP and mAHP, fast and medium AHPs following a single AP (truncated); Rec, recovery after BMI.

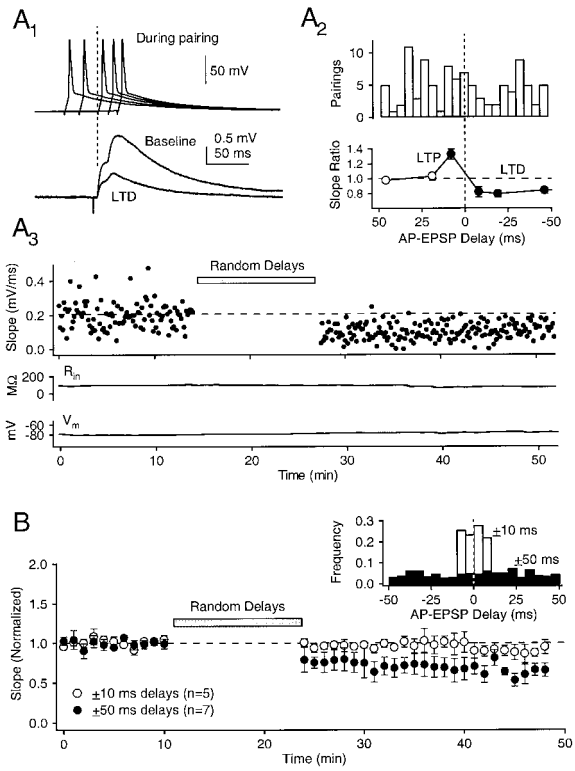

Figure 6. Depression of EPSPs Uncorrelated with Postsynaptic APs

(A) Example of LTD induced by randomly varying AP-EPSP delays (range of delays: −50 to +50 ms).

(A_1) Five consecutive postsynaptic APs evoked during pairing, relative to the mean baseline and postpairing EPSPs. Dashed line, EPSP onset.

(A_2) Actual distribution of AP-EPSP delays during pairing for this cell, relative to the windows for LTP and LTD (from Figure 5).

(A_3) EPSP slope for each sweep of the experiment. Pairing with random delays induced LTD (EPSP slope ratio: 0.45).

(B) Mean effect of pairing with random delays. Seven cells were tested with delays that varied randomly from −50 to +50 ms (closed circles), and five cells were tested with delays that varied from −10 to +10 ms (open circles).

(Inset) Actual distribution of pairing delays across all cells for each group.

tion of timing-based plasticity. Additional experiments were performed in slices that had not been exposed to BMI (Figure 5C). In these experiments, layer IV stimulation evoked compound PSPs usually containing both excitatory and inhibitory components, as determined by recording at resting (−75 mV) and depolarized (−50 mV) potentials (E_{Cl}: −70 mV). IPSPs were evident as hyperpolarizations at −50 mV. Analysis was restricted to the initial slope of PSPs that had an initial excitatory component. Under these conditions, pairing delays of +10 ms resulted in LTP (mean slope ratio: 1.20 ± 0.05, n = 4), and pairing delays of −20 ms resulted in LTD (0.85 ± 0.04, n = 5). LTP and LTD were significant across the population (LTP: $p < 0.05$, LTD: $p < 0.05$, two-tailed, one-sample t test) but were somewhat smaller in magnitude than when BMI was present (LTP: 1.33 ± 0.07, n = 10; LTD: 0.80 ± 0.04, n = 13). Thus, disinhibition is not required for induction of LTP and LTD by AP-EPSP pairing, though it may increase the magnitude of plasticity.

Recently, it was shown that BMI directly blocks Ca^{2+}-dependent afterhyperpolarizations (AHPs) in some cells (Debarbieux et al., 1998) and therefore could delay repolarization after the AP and potentially change the window for LTD induction. To determine if the long LTD window at this synapse was a result of BMI blocking the AHP, AP-EPSP pairing was performed in a separate group of cells using picrotoxin (PTX) to block $GABA_A$ currents instead of BMI. PTX does not block AHPs (Debarbieux

et al., 1998). First, it was shown that BMI partially inhibited the medium AHP (mAHP) in these cells, while PTX did not (Figure 5D, top). Across cells, BMI (50 μM, bath applied) reversibly reduced the mAHP following a single action potential to 74% ± 6% of control amplitude (n = 8), whereas PTX (50 μM) had no effect (101% ± 6% of control, n = 8). Neither drug blocked the fast AHP. Next, AP-EPSP pairing at −50 ms delays was performed in the presence of focally applied PTX (5 mM in a 5–6 μm tip pipette located 40–95 μm from soma) instead of BMI. Pairing produced significant LTD (mean slope ratio: 0.87 ± 0.05, n = 9, $p < 0.02$, two-tailed t test versus 1.0 mean), demonstrating that the long window for LTD was not due to the modest effect of BMI on the AHP (Figure 5D, bottom).

Discussion

These results demonstrate that excitatory vertical inputs onto layer II/III pyramids exhibit LTP and LTD based on the precise timing of EPSPs and postsynaptic APs. Timing-based plasticity was NMDA receptor dependent and could be induced by transient changes in AP-EPSP timing. LTP was induced when EPSPs led APs within a narrow temporal window (AP-EPSP delays up to 15 ms), and LTD was induced when APs led EPSPs within a broader window up to 50 ms long (Figure 5). This long temporal window for LTD induction is unusual among timing-based learning rules (Bi and Poo, 1998; Debanne et al., 1998; Zhang et al., 1998; Egger et al., 1999) and has the consequence that EPSPs uncorrelated with postsynaptic spiking become depressed over time (Figure 6).

LTP and LTD were observed at vertical synapses in layer II/III over an age range spanning from postnatal day 15 to postnatal day 31 (P15–P31). In contrast, LTP and LTD can be induced at thalamocortical synapses in layer IV of S1 only during an early developmental period ending at P7–P8 (Crair and Malenka, 1995; Feldman et al., 1998). This age dependence for LTP and LTD correlates with layer-specific critical periods for experience-dependent plasticity: in layer IV, plasticity in response to altered patterns of whisker input is most robust during an early critical period ending at P4–P6, whereas in layer II/III, plasticity persists through at least 1 year of age (Fox, 1992; Diamond et al., 1993, 1994; Armstrong-James et al., 1994; Glazewski and Fox, 1996).

LTP and LTD Induced by Postsynaptic Depolarization

In S1, homosynaptic LTP and LTD can be induced at vertical inputs to layer II/III by high- and low-frequency stimulation, respectively, of layer IV (Aroniadou-Anderjaska and Keller, 1995; Castro-Alamancos et al., 1995; Kitagawa et al., 1997). These protocols are thought to induce LTP or LTD by depolarizing the postsynaptic cell to different levels, thereby producing different postsynaptic Ca^{2+} signals, which, in turn, trigger LTP or LTD (Lisman, 1989; Artola et al., 1990; Cummings et al., 1996; Hansel et al., 1997). Consistent with this model, LTP and LTD were shown in this study to be induced by different levels of postsynaptic depolarization, irrespective of stimulation frequency (Figure 2). However, it seems unlikely that prolonged high- or low-frequency firing drives plasticity in S1 in vivo, since sensory stimuli typically modulate baseline firing rates in S1 by only a single spike per whisker deflection or whisking cycle (Simons, 1978; Fee et al., 1997). An alternative hypothesis, discussed below, is that sensory-driven changes in the temporal patterning of spikes in pre- and postsynaptic neurons may induce plasticity via timing-based LTP and LTD.

Timing-Based LTP and LTD

Long-term plasticity induced by the precise timing of EPSPs and postsynaptic APs has been described at several synapses (Bell et al., 1997; Magee and Johnston, 1997; Bi and Poo, 1998; Debanne et al., 1998; Zhang et al., 1998), including synapses in S1 between neighboring layer V pyramidal cells (Markram et al., 1997) and between neighboring layer IV stellate cells (Egger et al., 1999). Timing-based learning rules are Hebbian in nature and have computationally useful properties, such as resistance to saturation of synaptic weight, that simpler, correlation-based learning rules do not (Sejnowski, 1999).

A central feature of timing-based plasticity is the learning rule defined by the relationship between AP-EPSP pairing delay and magnitude of LTP or LTD. This learning rule differs across synapses. At retinotectal synapses and in dissociated hippocampal cell culture, LTP is induced by small positive pairing delays of up to ~20 ms (EPSPs leading APs), and LTD is induced in a symmetric window of small negative pairing delays (APs leading EPSPs; Bi and Poo, 1998; Zhang et al., 1998). Other synapses exhibit a similar, short (~20 ms) window for LTP, but a markedly longer window for LTD, extending to pairing delays of up to −50 or −100 ms (Debanne et al., 1998; the current study). Still other synapses exhibit fundamentally different temporal learning rules (Bell et al., 1997; Egger et al., 1999), suggesting that plasticity may be specialized to perform distinct functions at different synapses.

The learning rule in Figure 5 predicts that vertical inputs that are active immediately before postsynaptic APs and therefore contribute to pyramidal cell spiking will be strengthened, while synapses that are active after postsynaptic APs will be weakened. This behavior is characteristic of any learning rule in which positive delays lead to LTP and negative delays lead to LTD. The unusually long temporal window for LTD induction confers a second, unexpected property: because the integral of the LTD window is larger than that of the LTP window, EPSPs that are temporally uncorrelated or poorly correlated with postsynaptic spiking will, over time, elicit more LTD than LTP, and, therefore, synapses generating uncorrelated EPSPs will depress. Consistent with this prediction, when AP-EPSP delays were varied randomly over a broad range of values encompassing both LTP and LTD windows, robust LTD resulted (Figure 6). Depression of uncorrelated EPSPs is not expected for timing-based learning rules with LTP and LTD windows that have essentially equal integrals (e.g., Zhang et al., 1998), because over time, random pairing delays will generate equal amounts of LTP and LTD.

What cellular specialization could be responsible for the long LTD window at vertical synapses onto layer II/III pyramids? Timing-based LTP and LTD are thought to be triggered by a dendritic Ca^{2+} signal generated by interaction of the EPSP with the postsynaptic AP as it backpropagates into the local dendrites (Magee and Johnston, 1997). Several lines of evidence support the model that when the EPSP precedes the AP, a large Ca^{2+} signal is generated that is a supralinear sum of the

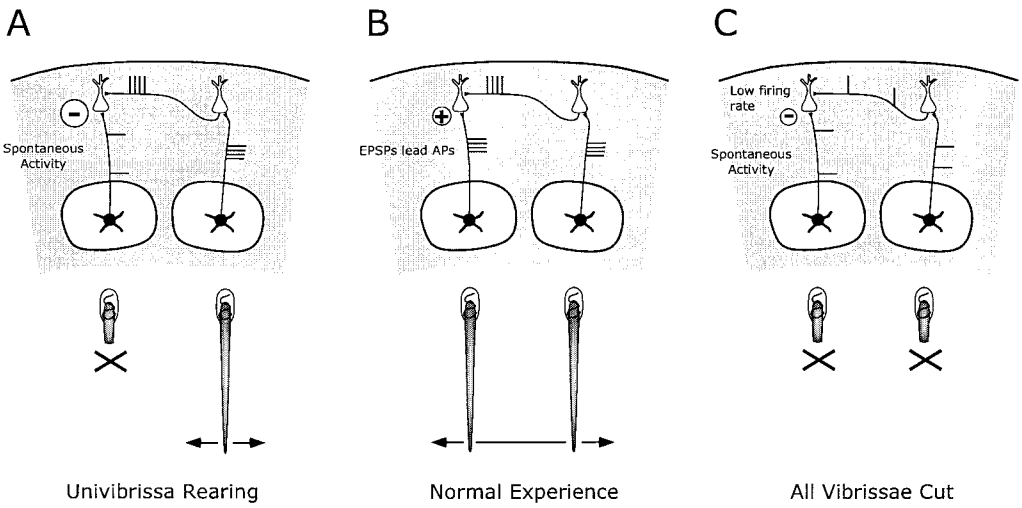

Figure 7. Model for Timing-Based LTP and LTD during Univibrissa Rearing

Each panel shows two neighboring barrel columns in S1, representing adjacent whiskers. Only layers I–IV are shown. White ovals represent barrels in layer IV. Ticks on schematic axons represent hypothesized patterns of AP firing.

(A) Univibrissa rearing. Vertical pathways in the deprived barrel column are assumed to be spontaneously active, and spontaneous activity is hypothesized to be poorly correlated with postsynaptic spiking and therefore to drive depression (minus sign) via the learning rule in Figure 5.

(B) Normal whisker experience. All pathways show whisker-evoked activity. Firing of layer IV cells drives firing of layer II/III neurons in each column, resulting in small, positive AP-EPSP delays. Circled plus sign, hypothesized LTP.

(C) All whiskers cut. All pathways are spontaneously active. Low firing rates in layer II/III are hypothesized to lead to fewer AP-EPSP pairings and therefore less LTD (small minus sign). See text for details.

Ca^{2+} signals produced by the EPSP or the AP alone, and LTP is induced. In contrast, when the AP precedes the EPSP, a smaller, sublinear Ca^{2+} signal is generated, and LTD is induced (Linden, 1999). Why a smaller Ca^{2+} signal is generated when the spike precedes the EPSP is unknown. However, the time course of dendritic repolarization following the backpropagating AP, the types of Ca^{2+} sources in the local dendrite, and the properties of local Ca^{2+} buffers may all influence the time course of the Ca^{2+} signal and therefore the window for LTD. Layer II/III pyramids are different from layer V and CA1 hippocampal pyramids in several of these respects and thus may be expected to display different plasticity windows (Helmchen et al., 1999; Kondo et al., 1999; Svoboda et al., 1999).

Implications for Experience-Dependent Plasticity in S1

This timing-based learning rule provides a simple explanation for the depression of deprived sensory responses in primary sensory cortex. Recall that during univibrissa rearing, principal whisker responses are rapidly depressed in layer II/III of deprived barrel columns in S1 and that this depression has been proposed to reflect LTD at excitatory vertical synapses from layer IV to layer II/III (Fox, 1992; Glazewski and Fox, 1996). During deprivation, layer IV cells in deprived columns are expected to lack principal whisker responses and most adjacent whisker responses but will remain spontaneously active (Simons and Land, 1987). Layer II/III cells in the same columns will lack principal whisker responses but will respond to the spared neighboring whisker due to input from excitatory intracolumnar pathways (Armstrong-James et al., 1992; Goldreich et al., 1999). If spontaneous spiking in layer IV is poorly correlated or uncorrelated with spontaneous and stimulus-driven spiking of layer II/III pyramids, the learning rule (Figure 5) predicts that vertical synapses will depress, because EPSPs at vertical synapses will be uncorrelated with postsynaptic spiking (Figure 6). This will cause depression of principal whisker responses (Figure 7A).

In contrast, depression should not occur in animals with normal whisker experience (Figure 7B). This is because principal whisker stimulation drives spiking in layer IV 2–4 ms before layer II/III (Armstrong-James et al., 1992), and, therefore, whisker-evoked EPSPs at vertical synapses will tend to lead postsynaptic APs. These positive AP-EPSP delays would be predicted to produce LTP, which would strengthen or stabilize those synapses and reinforce principal whisker responses.

This model also suggests why depression is less but still significant when all whiskers are deprived (Figure 7C). In this case, only spontaneous firing will occur. If spontaneous firing patterns in layer IV and layer II/III are poorly correlated, LTD will result, because vertical EPSPs will be poorly correlated with postsynaptic spikes. However, because postsynaptic firing rates will be lower than during univibrissa rearing, AP-EPSP pairing events will occur less frequently, and, therefore, less principal whisker depression should result. Conversely, when multiple whiskers are spared around a single deprived barrel column, layer II/III neurons in that column will have a high average firing rate due to convergent activation from neighboring whiskers. This should result in a large number of pairings with spontaneous vertical EPSPs and the greatest depression (Wallace and Fox, 1999). Thus, in this model, different amounts of spared whisker input produce varying amounts of depression on deprived pathways. This heterosynaptic-like behavior occurs because spared inputs modulate postsynaptic firing rate, which determines the frequency of AP-EPSP pairing events and therefore the rate at which plasticity is induced.

A central feature of this model is that spontaneous activity on pathways representing deprived sensory inputs must be poorly correlated with postsynaptic spiking in order to drive depression of those inputs. However, it is not currently known whether spontaneous activity in layer IV is, in fact, poorly correlated with spiking of layer II/III pyramids. Measuring this correlation in a behaving animal will be an important test of this hypothesis. A more general test for the involvement of timing-based learning rules in deprivation-induced plasticity is to determine whether acute deprivation alters millisecond scale firing correlations between synaptically connected cells (e.g., layer IV and layer II/III cells). If so, then deprivation-induced changes in spike timing could drive timing-based plasticity. However, if deprivation alters firing rates but not firing correlations, then classical, rate-based plasticity is more likely to be involved.

Implications for Ocular Dominance Plasticity in V1

Recently, it has been reported that the first step in ocular dominance plasticity in V1 is a rapid depression of closed eye responses in layer II/III (Mioche and Singer, 1989; Trachtenberg et al., 2000). As in S1, LTD on vertical pathways from layer IV to layer II/III may be involved (Cynader, 2000). If these inputs exhibit the same timing-based learning rule as in S1, then depression may result from an identical mechanism: as long as spontaneous activity on closed eye vertical pathways is poorly correlated with spiking of layer II/III cells driven by the open eye, LTD will be induced at vertical synapses, because the learning rule favors depression for uncorrelated inputs (Figures 5 and 6). As in S1, less depression is expected during binocular deprivation than during monocular deprivation (Wiesel and Hubel, 1965), because the firing rate of layer II/III cells will be lower when both eyes are closed, and, therefore, AP-EPSP pairings will occur less frequently. This does not exclude the involvement of a "sliding" plasticity threshold, which may further regulate the amount of LTD induced during different levels of average postsynaptic activity (Bienenstock et al., 1982; Bear et al., 1987).

Conclusions

The present results suggest that experience-dependent plasticity of cortical maps may be driven not just by average correlations between firing of different neurons, as hypothesized in most models of Hebbian plasticity (Bear et al., 1987; Miller et al., 1989; Benuskova et al., 1994; Fregnac et al., 1994) but also by the precise timing relationships between the firing of pre- and postsynaptic neurons. The timing-based learning rule observed for vertical inputs to layer II/III pyramids in S1 predicts that spontaneous activity, if it is poorly correlated with postsynaptic spiking, will drive depression of vertical inputs. This mechanism can explain several important aspects of map plasticity in S1 and V1.

Experimental Procedures

Coronal slices (400 μm) containing the posteromedial barrel subfield (PMBSF) were prepared from Long-Evans rats (P18–P32). Rats were anesthetized with halothane or isoflurane and decapitated, and the brain was rapidly removed in ice-cold Ringer solution (composition in mM: NaCl, 119; KCl, 2.5; $MgSO_4$, 1.3; NaH_2PO_4, 1; $NaHCO_3$, 26.3; D-(+)-glucose, 11; and $CaCl_2$, 2.5, bubbled with 95% O_2/5% CO_2 [pH 7.4]). Slices were cut on a vibrating microtome (Leica VT1000S), preincubated in Ringer solution at 31°C–34°C for 25 min, and then incubated at room temperature (20°C–23°C) until use (1–6 hr). Recordings were made at room temperature unless specified. For recordings at 32°C ± 1°C, the high temperature preincubation was omitted.

The PMBSF was identified by the presence of three to four large (250–450 μm diameter), barrel-like structures in layer IV, visible under transillumination. These structures correspond to whisker barrels, as labeled by cytochrome oxidase staining in the same slices (D. E. F., unpublished data; Finnerty et al., 1999). A concentric bipolar stimulating electrode (FHC, Bowdoinham, ME) was placed at the base of a layer IV barrel. Whole-cell recordings were made from layer II/III pyramidal cells in the same barrel column. A glass pipette (8–10 μm tip diameter) containing 5 mM BMI in Ringer solution was placed in layer II/III within 100 μm of the recording electrode in order to block $GABA_A$ receptors (Castro-Alamancos et al., 1995). Neurons with pyramidal shaped somata were selected for recording using infrared DIC optics. All cells exhibited regular spiking responses to positive current injection in current-clamp experiments, as expected for pyramidal cells (Connors and Gutnick, 1990; Agmon and Connors, 1992). Of 50 neurons randomly chosen for anatomical reconstruction using biocytin immunohistochemistry (Gottlieb and Keller, 1997), all were confirmed to be layer II/III pyramids.

Stimulation in layer IV evoked monosynaptic glutamatergic responses in layer II/III pyramidal cells (see Figure 1). These responses are interpreted as reflecting vertical, within-column inputs from layers IV–VI of the same barrel column, because these layers send major vertical projections to layer II/III (Lorente de No, 1922; Harris and Woolsey, 1979, 1983; Callaway, 1998). An alternative interpretation, that stimulation causes release from antidromically activated local axon collaterals of nearby II/III pyramids, is unlikely since antidromic action potentials were observed in only 2 of 305 pyramids (0.7%) with the stimulation intensities used to evoke EPSPs in this study (4–22 μA).

Whole-cell recordings were made with 3–4 MΩ pipettes using an Axopatch-1D amplifier (Axon). Sweeps were filtered at 2 kHz and digitized at 5 kHz using a 12 bit data acquisition board (National Instruments) and custom data acquisition and analysis routines running in Igor (Wavemetrics, Lake Oswego, OR).

Voltage-Clamp Experiments

The internal solution contained (in mM): cesium gluconate, 108; HEPES, 20; EGTA, 0.4; NaCl, 2.8; TEACl, 5; MgATP, 4; NaGTP, 0.3; and biocytin, 0.3% (w/v), adjusted to pH 7.25 with CsOH (290 mOsm). EPSCs were evoked at a constant rate of 0.1 or 0.167 Hz. After holding the cell at −70 mV for a baseline period of 8–15 min, plasticity was induced by holding the cell at either 0 mV or −50 mV for 50–100 stimuli without changing the stimulation rate. The holding potential was then returned to −70 mV. In LTP experiments, a short baseline (<8 min) was required to prevent dialysis of LTP. Series resistance (mean: 23 ± 9 MΩ [SD]) was calculated throughout the experiment from the whole-cell fast capacitative transient in response to a 5 mV hyperpolarization after compensation of the electrode fast capacitative transient (Isaac et al., 1995). Input resistance (mean: 260 ± 130 MΩ) was calculated from the sustained response to the same voltage step. Recordings were halted if the series or input resistance changed >30% over 50–60 min. EPSC amplitude was defined as the mean amplitude during a 2–3 ms window at the peak of the EPSC minus the amplitude during a similar window immediately before the stimulus artifact. Holding potentials were corrected for a measured junction potential of 10 mV.

Current-Clamp Experiments

The internal solution contained (in mM): potassium gluconate, 116; KCl, 6; NaCl, 2; HEPES, 20; EGTA, 0.5; MgATP, 4; NaGTP, 0.3; Na_2·phosphocreatine (Sigma, P-6502), 10; and biocytin, 0.3% (w/v), adjusted to pH 7.25 with KOH (300 mOsm). EPSPs were evoked at a constant rate of 0.1 or 0.133 Hz. The membrane potential was −74.6 ± 2.6 mV (SD), and cells depolarized by an average of 1.4 mV during 60 min of recording. Cells were excluded if they depolarized by more than 8 mV. Input resistance was calculated from the response to a hyperpolarizing current step during each sweep. The mean input resistance was 110 ± 35 MΩ (SD, range: 60–230 MΩ),

and the mean series resistance was 21 ± 10 MΩ (SD, range: 8–57 MΩ). Series resistance was compensated in current-clamp experiments. Stimulus intensity was set to evoke small, single component EPSPs or multicomponent EPSPs with an early component that was well separated from the rest of the response. The mean amplitude of the early component of the EPSP was 2.6 ± 1.2 mV (SD, n = 130 cells). Single postsynaptic action potentials were evoked by somatic current injection (mean: 1.4 ± 0.2 nA for 5–6 ms). The minimum current required to evoke an AP was used. For AP-EPSP pairing, the pairing interval was defined as the delay between the peak of the AP and the onset of the EPSP. Positive intervals correspond to EPSPs leading APs; negative intervals correspond to APs leading EPSPs. Only the initial slope (first 2–4 ms) of the EPSP was analyzed.

Quantification of LTP or LTD

Mean baseline slope or amplitude was calculated from 50 consecutive sweeps immediately before the start of pairing. Postpairing slope or amplitude was calculated from 50 sweeps beginning 10 min after the end of pairing. The amount of LTP or LTD was defined as the ratio of EPSP slope or amplitude in the postpairing period to that in the baseline. Only one pairing episode was applied to each cell.

D-APV Experiments

D-APV (50 μM; Tocris) was added to the Ringer solution continuously during the experiment.

Measurement of AHPs

Cells were depolarized to −49 ± 1 mV, and single APs were evoked by brief positive current injections (0.3–0.6 nA, 5 ms). The passive membrane response to an identical negative current pulse was subtracted to reveal the fast AHP (fAHP; mean: −4.1 mV) and mAHP (mean: −6.5 mV). BMI and PTX were bath applied. CNQX (10 μM) was present continuously. Recordings were made at room temperature.

Statistics

Comparisons were made by unpaired two-tailed Student's t test or ANOVA. The critical level of significance was $p < 0.05$. Means are reported ±SEM.

Acknowledgments

I thank Chris McBain for reading the manuscript. This work was supported by the intramural research program of the National Institute of Neurological Disorders and Stroke, National Institutes of Health.

Received April 14, 2000; revised May 26, 2000.

References

Agmon, A., and Connors, B.W. (1992). Correlation between intrinsic firing patterns and thalamocortical synaptic responses of neurons in mouse barrel cortex. J. Neurosci. *12*, 319–329.

Armstrong-James, M., Fox, K., and Das-Gupta, A. (1992). Flow of excitation within barrel cortex on striking a single vibrissa. J. Neurophysiol. *68*, 1345–1358.

Armstrong-James, M., Diamond, M.E., and Ebner, F.F. (1994). An innocuous bias in whisker use in adult rats modifies receptive fields of barrel cortex neurons. J. Neurosci. *14*, 6978–6991.

Aroniadou-Anderjaska, V., and Keller, A. (1995). LTP in the barrel cortex of adult rats. Neuroreport *6*, 2297–2300.

Artola, A., and Singer, W. (1993). Long-term depression of excitatory synaptic transmission and its relationship to long-term potentiation. Trends Neurosci. *16*, 480–487.

Artola, A., Brocher, S., and Singer, W. (1990). Different voltage-dependent thresholds for inducing long-term depression and long-term potentiation in slices of rat visual cortex. Nature *347*, 69–72.

Bear, M.F., Cooper, L.N., and Ebner, F.F. (1987). A physiological basis for a theory of synapse modification. Science *237*, 42–48.

Bell, C.C., Han, V.Z., Sugawara, Y., and Grant, K. (1997). Synaptic plasticity in a cerebellum-like structure depends on temporal order. Nature *387*, 278–281.

Benuskova, L., Diamond, M.E., and Ebner, F.F. (1994). Dynamic synaptic modification threshold: computational model of experience-dependent plasticity in adult rat barrel cortex. Proc. Natl. Acad. Sci. USA *91*, 4791–4795.

Bi, G., and Poo, M.-M. (1998). Synaptic modifications in cultured hippocampal neurons: dependence on spike timing, synaptic strength, and postsynaptic cell type. J. Neurosci. *18*, 10464–10472.

Bienenstock, E.L., Cooper, L.N., and Munro, P.W. (1982). Theory for the development of neuron selectivity: orientation specificity and binocular interaction in visual cortex. J. Neurosci. *2*, 32–48.

Buonomano, D.V., and Merzenich, M.M. (1998). Cortical plasticity: from synapses to maps. Annu. Rev. Neurosci. *21*, 149–186.

Callaway, E.M. (1998). Local circuits in primary visual cortex of the macaque monkey. Annu. Rev. Neurosci. *21*, 47–74.

Castro-Alamancos, M.A., Donoghue, J.P., and Connors, B.W. (1995). Different forms of synaptic plasticity in somatosensory and motor areas of the neocortex. J. Neurosci. *15*, 5324–5433.

Connors, B.W., and Gutnick, M.J. (1990). Intrinsic firing patterns of diverse cortical neurons. Trends Neurosci. *13*, 99–104.

Crair, M.C., and Malenka, R.C. (1995). A critical period for long-term potentiation at thalamocortical synapses. Nature *375*, 325–328.

Cummings, J.A., Mulkey, R.M., Nicoll, R.A., and Malenka, R.C. (1996). Ca^{2+} signaling requirements for long-term depression in the hippocampus. Neuron *16*, 825–833.

Cynader, M. (2000). Strengthening visual connections. Science *287*, 1943–1944.

Debanne, D., Gahwiler, B.H., and Thomson, S.M. (1998). Long-term synaptic plasticity between pairs of individual CA3 pyramidal cells in rat hippocampal slice cultures. J. Physiol. *507*, 237–247.

Debarbieux, F., Brunton, J., and Charpak, S. (1998). Effect of bicuculline on thalamic activity: a direct blockade of I_{AHP} in reticularis neurons. J. Neurophysiol. *79*, 2911–2918.

Diamond, M.E., Armstrong-James, M., and Ebner, F.F. (1993). Experience-dependent plasticity in adult rat barrel cortex. Proc. Natl. Acad. Sci. USA *90*, 2082–2086.

Diamond, M.E., Huang, W., and Ebner, F.F. (1994). Laminar comparison of somatosensory cortical plasticity. Science *265*, 1885–1888.

Egger, V., Feldmeyer, D., and Sakmann, B. (1999). Coincidence detection and changes of synaptic efficacy in spiny stellate neurons in rat barrel cortex. Nat. Neurosci. *2*, 1098–1105.

Fee, M.S., Mitra, P.P., and Kleinfeld, D. (1997). Central versus peripheral determinants of patterned spike activity in rat vibrissa cortex during whisking. J. Neurophysiol. *78*, 1144–1149.

Feldman, D.E., Nicoll, R.A., Malenka, R.C., and Isaac, J.T.R. (1998). Long-term depression at thalamocortical synapses in developing rat somatosensory cortex. Neuron *21*, 347–357.

Finnerty, G.T., Roberts, L.S., and Connors, B.W. (1999). Sensory experience modifies the short-term dynamics of neocortical synapses. Nature *400*, 367–371.

Fox, K. (1992). A critical period for experience-dependent synaptic plasticity in rat barrel cortex. J. Neurosci. *12*, 1826–1838.

Fregnac, Y., Burke, J.P., Smith, D., and Friedlander, M.J. (1994). Temporal covariance of pre and postsynaptic activity regulates functional connectivity in the visual cortex. J. Neurophysiol. *71*, 1403–1421.

Glazewski, S., and Fox, K. (1996). Time course of experience-dependent synaptic potentiation and depression in barrel cortex of adult rats. J. Neurophysiol. *75*, 1714–1729.

Glazewski, S., McKenna, M., Jacquin, M., and Fox, K. (1998). Experience-dependent depression of vibrissa responses in adolescent barrel cortex. Eur. J. Neurosci. *10*, 2107–2116.

Goldreich, D., Kyriazi, H.T., and Simons, D.J. (1999). Functional independence of layer IV barrels in rodent somatosensory cortex. J. Neurophysiol. *82*, 1311–1316.

Gottlieb, J.P., and Keller, A. (1997). Intrinsic circuitry and physiological properties of pyramidal neurons in rat barrel cortex. Exp. Brain Res. *115*, 47–60.

Hansel, C., Artola, A., and Singer, W. (1997). Relation between dendritic Ca^{2+} levels and the polarity of synaptic long-term modifications in rat visual cortex neurons. Eur. J. Neurosci. *9*, 2309–2322.

Harris, R.M., and Woolsey, T.A. (1979). Morphology of Golgi-impregnated neurons in mouse cortical barrels following vibrissae damage at different postnatal ages. Brain Res. *161*, 143–149.

Harris, R.M., and Woolsey, T.A. (1983). Computer-assisted analyses of barrel neuron axons and their putative synaptic targets. J. Comp. Neurol. *220*, 63–79.

Hebb, D.O. (1949). The Organization of Behavior (New York: J. Wiley and Sons).

Helmchen, F., Svoboda, K., Denk, W., and Tank, D.W. (1999). In vivo dendritic calcium dynamics in deep-layer cortical pyramidal neurons. Nat. Neurosci. *2*, 989–996.

Hestrin, S., Nicoll, R.A., Perkel, D.J., and Sah, D. (1990). Analysis of excitatory synaptic action in pyramidal cells using whole-cell recording from rat hippocampal slices. J. Physiol. *422*, 203–225.

Isaac, J.T.R., Nicoll, R.A., and Malenka, R.C. (1995). Evidence for silent synapses: implications for the expression of LTP. Neuron *15*, 427–434.

Kaas, J.H. (1991). Plasticity of sensory and motor maps in adult animals. Annu. Rev. Neurosci. *14*, 137–167.

Kitagawa, H., Nishimura, Y., Yoshioka, K., Lin, M., and Yamamoto, T. (1997). Long-term potentiation and depression in layer III and V pyramidal neurons in the cat sensorimotor cortex in vitro. Brain Res. *751*, 339–343.

Kondo, H., Tanaka, K., Hashikawa, T., and Jones, E.G. (1999). Neurochemical gradients along monkey sensory cortical pathways: calbindin-immunoreactive pyramidal neurons in layers II and III. Eur. J. Neurosci. *11*, 4197–4203.

Kossut, M. (1992). Plasticity of the barrel cortex neurons. Prog. Neurobiol. *39*, 389–422.

Lee, S.M., Weiskopf, M.G., and Ebner, F.F. (1991). Horizontal long-term potentiation of responses in rat somatosensory cortex. Brain Res. *544*, 303–310.

Linden, D.J. (1999). The return of the spike: postsynaptic action potentials and the induction of LTP and LTD. Neuron *22*, 661–666.

Lisman, J.E. (1989). A mechanism for the Hebb and anti-Hebb processes underlying learning and memory. Proc. Natl. Acad. Sci. USA *86*, 9574–9578.

Lorente de No, R. (1922). La corteza cerebral del raton. Trab. Lab. Invest. Biol. Madrid *20*, 41–78.

Magee, J.C., and Johnston, D. (1997). A synaptically controlled, associative signal for Hebbian plasticity in hippocampal neurons. Science *275*, 209–213.

Malenka, R.C., and Nicoll, R.A. (1993). NMDA-receptor-dependent synaptic plasticity: multiple forms and mechanisms. Trends Neurosci. *16*, 521–527.

Markram, H., Lubke, J., Frotscher, M., and Sakmann, B. (1997). Regulation of synaptic efficacy by coincidence of postsynaptic APs and EPSPs. Science *275*, 213–215.

Miller, K.D., Keller, J.B., and Stryker, M.P. (1989). Ocular dominance column development: analysis and simulation. Science *245*, 605–615.

Mioche, L., and Singer, W. (1989). Chronic recordings from single sites of kitten striate cortex during experience-dependent modifications of receptive-field properties. J. Neurophysiol. *62*, 185–197.

Ngezahayo, A., Schachner, M., and Artola, A. (2000). Synaptic activity modulates the induction of bidirectional synaptic changes in adult mouse hippocampus. J. Neurosci. *20*, 2451–2458.

Rittenhouse, C.D., Shouval, H.Z., Paradiso, M.A., and Bear, M.F. (1999). Monocular deprivation induces homosynaptic long-term depression in visual cortex. Nature *397*, 347–350.

Sejnowski, T.J. (1999). The book of Hebb. Neuron *24*, 1–20.

Simons, D.J. (1978). Response properties of vibrissa units in rat S1 somatosensory cortex. J. Neurophysiol. *41*, 798–820.

Simons, D.J., and Land, P.W. (1987). Early experience of tactile stimulation influences organization of somatic sensory cortex. Nature *326*, 694–697.

Singer, W. (1995). Development and plasticity of cortical processing architectures. Science *270*, 758–764.

Stent, G.S. (1973). A physiological mechanism for Hebb's postulate of learning. Proc. Natl. Acad. Sci. USA *95*, 3245–3250.

Svoboda, K., Helmchen, F., Denk, W., and Tank, D.W. (1999). Spread of dendritic excitation in layer 2/3 pyramidal neurons in rat barrel cortex in vivo. Nat. Neurosci. *2*, 65–73.

Trachtenberg, J.T., Trepel, C., and Stryker, M.P. (2000). Rapid extragranular plasticity in the absence of thalamocortical plasticity in the developing visual cortex. Science *287*, 2029–2032.

Wallace, H., and Fox, K. (1999). The effect of vibrissa deprivation pattern on the form of plasticity induced in rat barrel cortex. Somatosens. Motor Res. *16*, 122–138.

Wang, X., Merzenich, M.M., Sameshima, K., and Jenkins, W.M. (1994). Remodeling of hand representation in adult cortex determined by timing of tactile stimulation. Nature *378*, 71–75.

Wiesel, T.N., and Hubel, D.H. (1965). Comparison of the effects of unilateral and bilateral eye closure on cortical unit responses in kittens. J. Neurophysiol. *40*, 891–903.

Zhang, L.I., Tao, H.W., Holt, C.E., Harris, W.A., and Poo, M.-M. (1998). A critical window for cooperation and competition among developing retinotectal synapses. Nature *395*, 37–44.